April 9-2012

HYDROGEN BONDING IN THE CRYSTAL STRUCTURE OF LEGRANDITE: $Zn_2(AsO_4)(OH)(H_2O)$

Frank C. Hawthorne* & Yassir Abdu

Department of Geological Sciences, University of Manitoba,

Winnipeg, Manitoba, Canada R3T 2N2

Kimberly T. Tait

Department of Natural History, Royal Ontario Museum, 100 Queen's Park, Toronto,

Ontario M5S 2C6, Canada

* email: frank_hawthorne@umanitoba.ca

ABSTRACT

The crystal structure of legrandite: $Zn_2(AsO_4)(OH)(H_2O)$, monoclinic, *a* 12.8052(3), *b* 7.9249(2), *c* 10.2173 (2) Å, β 104.4329(3)°, V 411.0 Å^3, space group $P2_1/c$, Z = 2, has been refined to an R_1 value of 1.2% based on 2844 unique [$|F_o| > 4\sigma F$] reflections measured with a Bruker D8 three-circle diffractometer equipped with a rotating-anode generator (Mo*K*α X-radiation), multilayer optics and an APEX-II detector. The legrandite structure is a heteropolyhedral framework of (AsO_4) tetrahedra, ($Zn\varphi_5$) square pyramids and ($Zn\varphi_6$) octahedra [φ = O, (OH), (H_2O)] with extensive hydrogen bonding across its interstices. All hydrogen positions were located, all hydrogen bonds were assigned, and the H...O distances are in reasonable accord with the published relation between O-H stretching frequency and H...O bond-length.

Keywords: legrandite, crystal-structure, electron-microprobe analysis, hydrogen bonding.

INTRODUCTION

There has been much work in the last twenty years on developing hierarchical classifications of oxysalt minerals (Hawthorne 1984, 1985, 1986, 1990, 1997, Sabelli & Trosti-Ferroni 1985, Hawthorne *et al.* 1996, 2000, Hawthorne & Huminicki 2002, Huminicki & Hawthorne 2002, Burns 1999, Burns *et al.* 1996, Krivovichev 2005, 2008, Krivovichev & Filatov 1999), focusing on the bond topology of the more strongly bonded cations. With much of this work now in place for minerals, it is important to focus on the bond topology of the interstitial species (e.g., Schindler & Hawthorne 2001a,b,c, 2004, 2008, Schindler *et al.* 2006). It is the interstitial bonds that control the stability of minerals, as these weak bonds are more easily broken with changing conditions than the stronger bonds of the structural unit. Hydrogen bonds are of particular importance in this regard, and the stabilities of a large number of oxysalt minerals are controlled by the weak hydrogen bonds that bind their structural units together. Consequently it is important to determine the details of hydrogen bonding in oxysalt minerals if we are to understand the details of their stability and the mechanisms by which they break down. With this as background, here we describe the pattern of hydrogen bonding in legrandite.

EXPERIMENTAL

The crystal used in this work come from the Tsumeb mine, Otjikoto (Oshikoto) region, Namibia, and was taken from the holotype sample for ianbruceite (Cooper *et al*. 2012).

Collection of X-ray intensity data

A single crystal on a tapered glass fibre was mounted on a Bruker D8 three-circle diffractometer equipped with a rotating-anode generator (Mo*K*α), multilayer optics and an APEX-II detector. A total of 10,229 intensities (3358 within the Ewald sphere) was collected to 60° 2θ using 40 s per 0.3° frames with a crystal-to-detector distance of 8 cm. Empirical

absorption corrections (SADABS; Sheldrick 2008) were applied and equivalent reflections were then corrected for Lorentz, polarization and background effects, averaged and reduced to structure factors. The unit cell dimensions were obtained by least-squares refinement of the positions of 4921 reflections with $I > 10\sigma(I)$ and are given in Table 1, together with other information pertaining to data collection and structure refinement.

Crystal-structure refinement

All calculations were done with the SHELXTL PC (Plus) system of programs. Systematic absences in the single-crystal X-ray diffraction data are consistent with space group $P2_1/c$, and the structure was solved with this symmetry. Crystal-structure refinement was initiated with the atom coordinates of McLean *et al.* (1971), and the structure was refined by full-matrix least-squares to an R_1 index of 1.2%. At the final stages of refinement, six H (hydrogen) sites were identified in difference-Fourier maps and were inserted into the refinement. The O(donor)-H differences were softly constrained to be close to 0.98 Å and the H-H distances were softly constrained to be close to 1.59 Å during refinement. Refined atom coordinates and anisotropic-displacement parameters are listed in Table 2, selected interatomic distances are given in Table 3, and bond valences, calculated with the parameters of Brown & Altermatt (1985), are given in Table 4. Bond-valences for hydrogen bonds were calculated from the curve of Brown (1976). A table of structure-factors and a cif file may be obtained from The Depository of Unpublished Data, on the MAC website [document Legrandite CM-------].

Electron-microprobe analysis

Several crystals of legrandite of differing shades of blue were mounted in epoxy on 2.5 cm diameter Perspex discs, ground, polished, carbon-coated and analyzed with a Cameca SX-100 electron microprobe operating under the following conditions in wavelength-dispersion

mode: excitation voltage: 15 kV, specimen current: 10 nA, beam size: 10 μm, peak count-time: 20 s, background count-time: 20 s. We used the following standards and crystals for *K*α X-ray lines: Zn, As: adamite; Fe: fayalite; Mn: spessartine. Chemical formulae were calculated on the basis of six anions with one (OH) group and one (H_2O) group. The chemical compositions and unit formulae are given in Table 5.

Infrared spectroscopy

The FTIR spectrum was collected using a Bruker Tensor 27 FTIR spectrometer equipped with a KBr beam splitter and a DLATGS detector. Spectra over the range 4000-400 cm^{-1} was obtained by averaging 100 scans with a resolution of 4 cm^{-1}. Base-line correction was done using the OPUS spectroscopic software (Bruker Optic GmbH). The spectrum is shown in Figure 1.

DESCRIPTION OF THE STRUCTURE

Cation polyhedra

Each cation polyhedron is labelled by its central cation site. There are two distinct *As* sites, each occupied by As^{5+}, as indicated by the site scattering, and tetrahedrally coordinated by O anions with <*As*-O> distances of 1.687 and 1.683 Å, close to values previously reported for <As^{5+}-O> distances, *e.g.*, 1.680 in scorodite (Hawthorne 1976a), 1.681 Å in adamite (Hawthorne 1976b) and 1.685 Å in brandtite (Herwig & Hawthorne 2006). There are four distinct *Zn* sites, all of which are occupied by Zn, as indicated by the site scattering at each site. *Zn*(1) is octahedrally coordinated by O anions with a <*Zn*-O> distance of 2.111 Å. *Zn*(2), *Zn*(3) and *Zn*(4) are [5]-coordinated by O anions with <*Zn*-O> distances of 2.032, 2.078 and 2.044 Å.

Bond topology

The polyhedron linkage is quite complicated in legrandite, as is commonly the case in minerals in which the divalent cations are [5]-coordinated. Two *Zn*(1) octahedra share an edge (Fig. 2) and the vertices *cis* to this edge are linked by *As*(2) tetrahedra, forming an $[M_2\Phi_6(TO_4)_2]$ cluster (Φ is an unspecified anion) that Hawthorne (1983) showed is one of the four clusters of two octahedra and two tetrahedra that show optimum agreement with the valence-sum rule. This cluster links to other clusters of the same sort by sharing vertices between octahedra and tetrahedra to form a sheet (Fig. 3a) with alternate chains of clusters tilted in opposite directions (Fig. 3b).

The *Zn*(2) and *Zn*(4) polyhedra share an edge to form a dimer, and the dimer shares a corner with the *Zn*(3) polyhedron to form a trimer (Fig. 4), and these trimers form a disconnected layer parallel to (100) (Fig. 4). This layer is quite corrugated (Fig. 5a), and two of these layers, facing in opposite directions, sandwich the *Zn*(1)-*As*(2) layer (Fig. 3) as shown in Figure 5b. The result is a very thick layer (Fig. 5b) parallel to (100), with *Zn*(4) polyhedra projecting from both sides of the sheet. These sheets stack in the **a** direction such that the projecting *Zn*(4) polyhedra fit into the staggered gaps in the opposing later (Fig. 5). The layers are linked in the **a** direction by *As*(1) tetrahedra (Fig. 5a) and hydrogen bonding (Fig. 5b).

Interstitial hydrogen-bond arrangements

The stereochemical details of the hydrogen bonding are given in Table 3. There are two (OH) groups [O(10) and O(11)] and two (H_2O) groups [O(9) and O(12)]. The environment of the two (OH) groups is shown in Figure 6. Both H(1) and H(2) project into a cavity enclosed by the Zn(1), *Zn*(2) and *Zn*(3) polyhedra. The H(1) atom is 2.86 Å from the O(8) anion; is this a hydrogen bond? Brown (1976) has examined hydrogen bonding in a series of perchloric-acid hydrates: $H(ClO_4)(H_2O)_n$ (n = 1, 2, 2.5, 3, 3.5). These compounds are of particular interest as

the perchlorate groups are held together only by hydrogen bonds. Brown (1976) used the valence-sum rule (Brown 2002) to show that hydrogen separations up to 3.1 Å are significant hydrogen bonds. Thus the H(1)…O(8) distance of 2.86 A constitutes a hydrogen bond, even though it is significantly longer that the other hydrogen bonds in the legrandite structure. The H(2) atom is 1.96 Å from the O(8) anion (Table 3), indicating a much stronger hydrogen bond than that involving H(1).

Figure 7a shows the part of the structure where the sheets in Figure 5b join together. The environment of the two (H_2O) groups is shown in Figure 7b, the same part of the structure as that shown in Figure 7a but with the arsenate groups removed for clarity. The (H_2O) groups attach to the *Zn*(4) polyhedron and form a convoluted sheet (seen end-on in Fig. 7b) through the structure. The detailed stereochemistry around the two (H_2O) groups is shown in Figure 8. The O(donor)-H distances are all in the most common range for hydrogen bonds (1.65-2.08 Å) and the O(donor)-H...O(acceptor) angles are all close to 165°.

Hydrogen bonding and the infrared spectrum

Inspection of the H...O bond-lengths (Table 3) shows that they vary in the range 1.66-2.86 Å. It is well-known (*e.g*., Libowitzky 1999) that the principal O-H stretching frequency in the infrared is strongly correlated with the H...O distance in inorganic materials, and the wide range in H...O bond-lengths in legrandite should be reflected in its infrared spectrum. Inspection of Figure 1 shows this to be the case: the principal bands show absorption frequencies from 3574 to 2882 cm^{-1}. The bands from (OH) groups are generally much narrower than bands from (H_2O) groups, and broaden with decreasing absorption frequency (*e.g*., Groat *et al*. 1995). This allows us to assign the bands as follows: 3574 cm^{-1}: O(10)-H(1); 3304 cm^{-1}: O(11)-H(2); 3113 cm^{-1}: O(9) (H_2O); 2882 cm^{-1}: O(12) (H_2O). As shown in Figure 9, this assignment produces reasonable accord with the relation of Libowitzky (1999).

A note on the colour of legrandite

Legrandite is normally bright yellow. However, the legrandite (from the Tsumeb mine) used in this work is colourless to pale blue. Initially, we suspected the presence of minor Cu, but chemical analysis (Table 5) showed this not to be the case: we could not detect Cu in either sample. Inspection of the formulae (Table 5) shows a slightly higher Fe content in the pale-blue crystals, and this is presumably the origin of the pale-blue colour.

ACKNOWLEDGEMENTS

We thank Mark Cooper for his help with the experimental part of this work. This work was supported by a Canada Research Chair in Crystallography and Mineralogy, Research Tools and Equipment, Major Facilities Access and Discovery Grants from the Natural Sciences and Engineering Research Council of Canada and Canada Foundation for Innovation Grants to FCH.

REFERENCES

Brown, I.D. (1976): Hydrogen bonding in perchloric acid hydrates. *Acta Crystallogr.* **A32**, 786-792.

Brown, I.D. (2002): The chemical bond in inorganic chemistry. The bond valence model. Oxford University Press.

Brown, I.D. & Altermatt, D. (1985): Bond-valence parameters obtained from a systematic analysis of the inorganic crystal structure database. *Acta Crystallogr.* **B41**, 244-247.

Burns, P.C. (1999): The crystal chemistry of uranium. *Rev. Mineral.* **38**, 23-90.

Burns, P.C., Miller, M.L. & Ewing, R.C. (1996): U^{6+} minerals and inorganic phases: A comparison and hierarchy of structures. *Can. Mineral.* **34**, 845-880.

Cooper, M.A., Abdu, Y.A., Ball, N.A., Hawthorne, F.C., Back, M.E., Tait, K.T., Schlüter, J., Malcherek, T., Pohl, D. & Gebhard, G. (2012): Ianbruceite, ideally $Zn_2(OH)(H_2O)(AsO_4)_2(H_2O)_2$, a new arsenate mineral from the Tsumeb Mine, Otjikoto (Oshikoto) Region, Namibia: Description and crystal structure. *Mineral. Mag.* (submitted)

Groat, L.A., Hawthorne, F.C., Rossman, G.R. & Ercit, T.S. (1995): The infrared spectroscopy of vesuvianite in the OH region. *Can. Mineral.* **33**, 609-626.

Hawthorne, F.C. (1976a): The hydrogen positions in scorodite. *Acta Crystallogr*. **B32**, 2891-2892.

Hawthorne, F.C. (1976b): A refinement of the crystal structure of adamite *Can Mineral*. **14**, 143-148.

Hawthorne, F.C. (1983): Graphical enumeration of polyhedral clusters. *Acta Crystallogr*. **A39**, 724-736.

Hawthorne, F.C. (1984): The crystal structure of stenonite, and the classification of the aluminofluoride minerals. *Can. Mineral.* **22**, 245-251.

Hawthorne, F.C. (1985): Towards a structural classification of minerals: The $^{VI}M^{IV}T_2\varphi_n$ minerals.

Am. Mineral. **70**, 455-473.

Hawthorne, F.C. (1986): Structural hierarchy in $^{VI}M_x^{III}T_y\varphi_z$ minerals. *Can*. *Mineral.* **24**, 625-642.

Hawthorne, F.C. (1990): Structural hierarchy in $^{[6]}M^{[4]}T\varphi_n$ minerals. *Z. Kristallogr.* **192**, 1-52.

Hawthorne, F.C. (1997): Structural aspects of oxide and oxysalt minerals. *In*: European Mineralogical Union Notes in Mineralogy, Vol.1, "Modular Aspects of Minerals" (S. Merlino, ed.). Eötvös University Press, 373-429.

Hawthorne, F.C. & Huminicki, D.M.C. (2002): The crystal chemistry of beryllium. *Rev. Mineral. Geochem.* **50**, 333-403.

Huminicki, D.M.C. & Hawthorne, F.C. (2002): The crystal chemistry of the phosphate minerals. *Rev. Mineral. Geochem.* **48**, 123-253.

Hawthorne, F.C., Burns, P.C., Grice, J.D. (1996): The crystal chemistry of boron. *Rev. Mineral.* **33**, 41-115.

Hawthorne, F.C., Krivovichev, S.V. & Burns, P.C. (2000): The crystal chemistry of sulfate minerals. *Rev. Mineral. Geochem.* **40,** 1-112.

Herwig, S. & Hawthorne, F.C. (2006): The topology of hydrogen bonding in brandtite, collinsite and fairfieldite. *Can. Mineral*. **44**, 1181-1196.

Krivovichev, S.V. (2005): Topology of microporous structures. *Rev. Mineral. Geochem*. **57**, 17-68.

Krivovichev, S.V. (2008): Structural Crystallography of Inorganic Oxysalts. Oxford University Press.

Krivovichev, S.V. & Filatov, S.K. (1999): Structural principles for minerals and inorganic compounds containing anion-centered tetrahedra. *Am. Mineral*. **84**, 1099-1106.

Libowitzky, E. (1999): Correlation of O-H stretching frequencies and O-H...O hydrogen bond lengths in minerals. *Monat. Chem*. **130**, 1047-1059.

McLean, W.J., Anthony, J.W., Finney, J.J. & Laughon, R.B. (1971): The crystal structure of

legrandite. *Am. Mineral.* **56**, 1147-1154.

Sabelli, C., Trosti-Ferroni, R. (1985): A structural classification of sulfate minerals. *Per. Mineral.* **54**, 1-46.

Schindler, M. & Hawthorne, F.C. (2001a): A bond-valence approach to the structure, chemistry and paragenesis of hydroxy-hydrated oxysalt minerals: I. Theory. *Can. Mineral.* **39**, 1225-1242

Schindler, M. & Hawthorne, F.C. (2001b): A bond-valence approach to the structure, chemistry and paragenesis of hydroxy-hydrated oxysalt minerals: II. Crystal structure and chemical composition of borate minerals. *Can. Mineral.* **39**, 1243-1256.

Schindler, M. & Hawthorne, F.C. (2001c): A bond-valence approach to the structure, chemistry and paragenesis of hydroxy-hydrated oxysalt minerals: III. Paragenesis of borate minerals. *Can. Mineral.* **39**, 1257-1274.

Schindler, M. & Hawthorne, F.C. (2004): A bond-valence approach to the uranyl-oxide hydroxy-hydrate minerals: Chemical composition and occurrence. *Can. Mineral.* **42**, 1601-1627.

Schindler, M. & Hawthorne, F.C. (2008): The stereochemistry and chemical composition of interstitial complexes in uranyl-oxysalt minerals. *Can. Mineral.* **46**, 467-501.

Schindler, M., Huminicki, D.M.C. & Hawthorne, F.C. (2006): Sulfate minerals: I. Bond topology and chemical composition. *Can. Mineral.* **44**, 1403-1429.

Sheldrick, G.M. (2008): A short history of *SHELX*. *Acta Crystallogr.* **A64**, 112-122.

FIGURE CAPTIONS

Fig. 1. The infrared spectrum of legrandite.

Fig. 2. The $[M_2\Phi_6(TO_4)_2]$ cluster (Φ is an unspecified anion) in legrandtite; *Zn*(1) octahedra are pale green, *As*(2) tetrahedra are orange.

Fig. 3. The $[M_2\Phi_6(TO_4)_2]$ clusters in legrandite, linked by sharing of vertices between *Zn* octahedra and *As* tetrahedra to form a sheet; (a) projected onto (100); (b) viewed parallel to the plane of the sheet. Legend as in Fig. 2.

Fig. 4. The disconnected layer of trimers of *Zn* octahedra in legrandite: *Zn*(2) and *Zn*(4) are yellow, *Zn*(3) is mauve.

Fig. 5. The intercalation of layers of polyhedra in legrandite projected onto (001); (a) the disconnected layer of trimers of *Zn* octahedra viewed edge-on; (b) the layer of $[M_2\Phi_6(TO_4)_2]$ clusters intercalated between two layers of Zn trimers. Legend as in Figs. 2 and 4.

Fig. 6. Details of the O(donor), H and O(acceptor) atoms and associated hydrogen bonds for the (OH) groups in legrandite. Legend as in Figs. 2 and 4, plus H atoms as red circles, O(donor)-H bonds as dark-blue lines, hydrogen bonds as broken green lines.

Fig. 7. (a) The *Zn*-*As* framework, omitting *Zn*(1) octahedra, in legrandite; (b) the corresponding *Zn* framework, showing the overall pattern of hydrogen bonds. Legends as in Figs. 2 and 4,

plus H atoms as green circles, O(donor)-H bonds as thin black lines, hydrogen bonds as red lines.

Fig. 8. Details of the O(donor), H and O(acceptor) atoms and associated hydrogen bonds for the (H_2O) groups in legrandite. Legend as in Fig. 6, the view is rotated slightly away from (001) to minimize overlap.

Fig. 9. Variation in principal OH-stretching frequency as a function of hydrogen-bondlength in legrandite; the curve is the relation of Libowitzky (1999).

TABLE 1. MISCELLANEOUS REFINEMENT DATA FOR LEGRANDITE

a (Å)	12.8052(3)
b	7.9249(2)
c	10.2173(2)
β(°)	104.4329(3)
V (Å^3)	1004.1( )
Space group	$P2_1/c$
Z	2
$D_{calc.}$ (g/cm^3)	4.030
Radiation/ filter	Mo$K\alpha$/graphite
2θ-range for data collection (°)	60.00
R(int) (%)	1.23
Reflections collected	11736
Independent reflections $F_o > 4\sigma F$	2943 2844
Final $R_{(obs)}$ (%) [$F_o > 4\sigma F$]	R_1 = 1.23
R indices (all data) (%)	R_1 = 1.34 wR_2 = 5.01 Goo*F* = 1.334

TABLE 2. ATOM POSITIONS AND DISPLACEMENT PARAMETERS (Å^2) FOR LEGRANDITE.

ATOM	*x*	*y*	*z*	U_{11}	U_{22}	U_{33}	U_{23}	U_{13}	U_{12}	U_{eq}
As(1)	0.14963(2)	0.05491(3)	0.21980(2)	0.00802(10)	0.00822(10)	0.00689(10)	-0.00034(7)	0.00203(7)	-0.00007(7)	0.00768(6)
As(2)	0.38529(2)	0.42165(3)	0.21410(2)	0.00833(10)	0.00779(10)	0.00740(10)	0.00019(7)	0.00278(7)	0.00002(7)	0.00770(6)
Zn(1)	0.40327(2)	0.04976(3)	0.38962(3)	0.01089(12)	0.01209(13)	0.01040(12)	0.00014(9)	0.00185(9)	0.00177(9)	0.01127(6)
Zn(2)	0.25255(2)	0.33083(3)	0.46242(3)	0.01025(12)	0.00927(12)	0.01152(12)	-0.00071(9)	0.00282(9)	0.00041(9)	0.01033(6)
Zn(3)	0.36202(2)	0.80578(3)	0.12765(3)	0.01449(13)	0.01042(12)	0.01209(12)	0.00182(9)	0.00046(10)	-0.00093(9)	0.01284(6)
Zn(4)	0.01007(2)	0.24192(4)	0.44038(3)	0.01113(12)	0.01557(13)	0.01250(13)	-0.00073(10)	0.00259(10)	-0.00091(9)	0.01313(7)
O(1)	0.26801(14)	0.9532(2)	0.26147(18)	0.0100(7)	0.0124(8)	0.0145(8)	-0.0022(6)	0.0005(6)	0.0030(6)	0.0127(3)
O(2)	0.13880(13)	0.1602(2)	0.07322(16)	0.0108(7)	0.0165(8)	0.0094(7)	0.0049(6)	0.0035(6)	0.0021(6)	0.0121(3)
O(3)	0.13303(13)	0.1895(2)	0.34154(17)	0.0114(7)	0.0152(8)	0.0127(7)	-0.0065(6)	0.0047(6)	-0.0019(6)	0.0128(3)
O(4)	0.04897(14)	0.9126(2)	0.20262(17)	0.0133(8)	0.0137(8)	0.0127(8)	-0.0023(6)	0.0036(6)	-0.0049(6)	0.0132(3)
O(5)	0.47910(13)	0.9513(2)	0.24071(17)	0.0090(7)	0.0164(8)	0.0129(7)	-0.0043(6)	0.0012(6)	0.0020(6)	0.0131(3)
O(6)	0.35330(14)	0.3422(2)	0.05675(16)	0.0178(8)	0.0168(8)	0.0085(7)	-0.0037(6)	0.0047(6)	-0.0080(7)	0.0141(3)
O(7)	0.34595(14)	0.2901(2)	0.31982(17)	0.0151(8)	0.0102(7)	0.0131(7)	0.0034(6)	0.0078(6)	0.0009(6)	0.0120(3)
O(8)	0.32021(15)	0.6062(2)	0.21800(18)	0.0220(9)	0.0096(7)	0.0193(8)	0.0037(6)	0.0124(7)	0.0051(7)	0.0157(3)
O(9)	0.07895(17)	0.5313(3)	0.1396(2)	0.0233(10)	0.0217(10)	0.0290(10)	0.0092(8)	0.0117(8)	0.0059(8)	0.0238(4)
O(10)	0.44584(14)	0.6626(2)	0.01455(17)	0.0128(7)	0.0112(7)	0.0116(7)	0.0002(6)	0.0037(6)	0.0003(6)	0.0118(3)
O(11)	0.27353(14)	0.5767(2)	0.46950(17)	0.0141(8)	0.0111(7)	0.0108(7)	-0.0009(6)	0.0040(6)	-0.0024(6)	0.0119(3)
O(12)	0.08807(16)	0.7338(3)	0.4346(2)	0.0199(9)	0.0294(10)	0.0193(9)	0.0088(8)	0.0101(7)	0.0090(8)	0.0219(4)
H(1)	0.461(4)	0.748(4)	-0.047(4)	0.05						
H(2)	0.267(4)	0.622(6)	0.379(2)	0.05						
H(3)	0.1576(4)	0.543(6)	0.163(5)	0.05						
H(4)	0.054(4)	0.468(5)	0.208(4)	0.05						
H(5)	0.060(4)	0.774(6)	0.3417(18)	0.05						
H(6)	0.150(2)	0.659(5)	0.444(5)	0.05						

TABLE 3. SELECTED INTERATOMIC DISTANCES (Å) AND ANGLES (°) IN LEGRANDITE

As(1)-O(1)a	1.676(2)	*As*(2)-O(5)b	1.698(2)
As(1)-O(2)	1.690(2)	*As*(2)-O(6)	1.679(2)
As(1)-O(3)	1.692(2)	*As*(2)-O(7)	1.667(2)
As(1)-O(4)a	1.689(2)	*As*(2)-O(8)	1.689(2)
<*As*(1)-O>	1.687	<*As*(2)-O>	1.683
Zn(1)-O(1)a	2.042(2)	*Zn*(2)-O(2)c	2.057(2)
Zn(1)-O(5)a	2.145(2)	*Zn*(2)-O(3)	2.045(2)
Zn(1)-O(6)c	2.145(2)	*Zn*(2)-O(6)c	1.963(2)
Zn(1)-O(7)	2.101(2)	*Zn*(2)-O(7)	2.128(2)
Zn(1)-O(10)c	2.100(2)	*Zn*(2)-O(11)	1.965(2)
Zn(1)-O(10)b	2.133(2)	<*Zn*(2)-O>	2.032
<*Zn*(1)-O>	2.111		
Zn(3)-O(1)	2.346(2)	*Zn*(4)-O(2)c	2.012(2)
Zn(3)-O(5)	2.012(2)	*Zn*(4)-O(3)	2.011(2)
Zn(3)-O(8)	1.972(2)	*Zn*(4)-O(4)e	2.113(2)
Zn(3)-O(10)	2.096(2)	*Zn*(4)-O(9)e	2.011(2)
Zn(3)-O(11)d	1.963(2)	*Zn*(4)-O(12)f	2.071(2)
<*Zn*(3)-O>	2.078	<*Zn*(4)-O>	2.044
O(11)-H(2)	0.980(1)	O(10)-H(1)	0.980(1)
H(2)....O(8)	1.93(3)	H(1)....O(8)	2.86(3)
O(11)-H(2)-O(8)	145(4)	O(10)-H(1)-O(8)	130(4)
O(12)-H(5)	0.980(1)	O(9)-H(3)	0.980(1)
O(12)-H(6)	0.980(1)	O(9)-H(4)	0.980(1)
H(5)....O(4)	1.77(2)	H(3)....O(8)	2.078(8)
H(6)....O(11)	1.666(12)	H(4)....O(4)e	1.83(2)
O(12)-H(5)-O(4)	156(4)	O(11)-H(2)-O(8)	171(4)
O(12)-H(6)-O(11)	165(4)	O(11)-H(2)-O(8)	152(4)

a: *x*, *y*-1, *z*; b: -*x*+1, *y*-½, -*z*+½; c: *x*, -*y*+½, *z*+½; d: *x*, -*y*+$^3/_2$, *z*-½; e: -*x*, *y*-½, -*z*+½; f: -*x*, -*y*+1, -*z*+1.

TABLE 4. BOND-VALENCE TABLE FOR LEGRANDITE*

	As(1)	*As*(2)	*Zn*(1)	*Zn*(2)	*Zn*(3)	*Zn*(4)	Σ'	H(1)	H(2)	H(3)	H(4)	H(5)	H(6)	Σ
O(1)	1.279		0.401		0.176		1.856							1.856
O(2)	1.231			0.385		0.435	2.051							2.051
O(3)	1.225			0.398		0.436	2.059							2.059
O(4)	1.235					0.331	1.566				0.17	0.19		1.962
O(5)		1.205	0.304		0.435		1.944							1.944
O(6)		1.268	0.304	0.497			2.069							2.069
O(7)		1.310	0.342	0.318			1.970							1.970
O(8)		1.235			0.485		1.720	0.02	0.15	0.12				2.030
O(9)						0.436	0.436			0.88	0.83			2.146
O(10)			0.343 0.314		0.347		1.004	0.98						1.984
O(11)				0.494	0.497		0.991		0.85				0.25	2.091
O(12)						0.371	0.371					0.81	0.75	1.911
Σ	4.970	5.028	2.008	2.092	1.940	2.009		1.00	1.00	1.00	1.00	1.00	1.00	

*calculated using the parameters of Brown & Altermatt (1985).

TABLE 5. CHEMICAL COMPOSITION (wt%) AND UNIT-CELL CONTENT (*apfu*)

	Colourless	Pale blue		Colourless	Pale blue
As_2O_5	37.73	37.16	As	1.004	1.005
ZnO	52.51	51.50			
FeO	0.10	0.24	Zn	1.973	1.967
MnO	0.28	0.22	Mn^{2+}	0.012	0.010
H_2O	8.84	8.69	Fe^{2+}	0.004	0.010
Sum	99.46	97.81	Sum	1.989	1.987
			OH	1	1
			H_2O	1	1

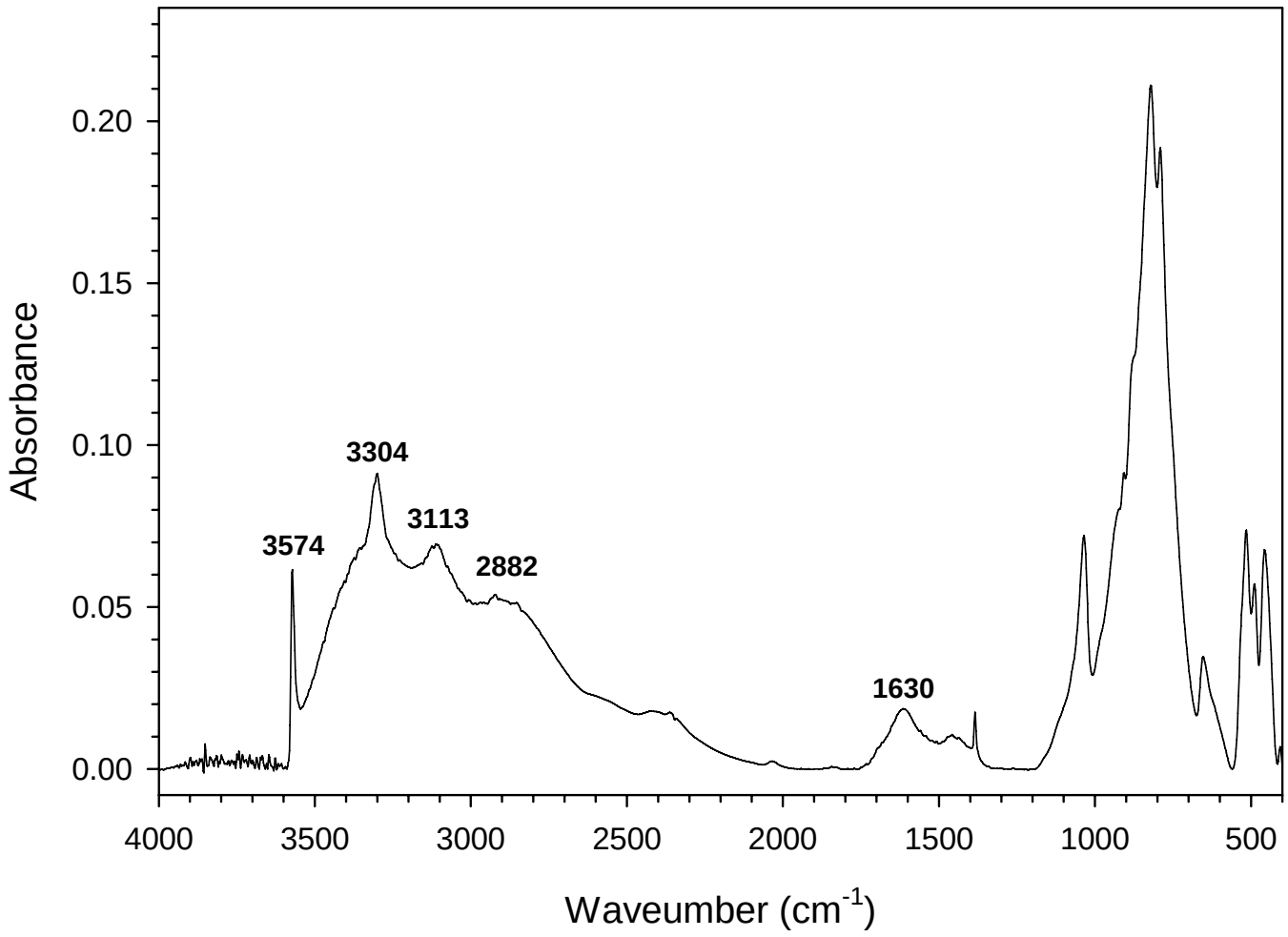
Absorbance
0.20
0.15
0.10
0.05
0.00
3574
3304
3113
2882
1630
4000
3500
3000
2500
2000
1500
1000
500
Waveumber (cm-1)

FIGURE 1

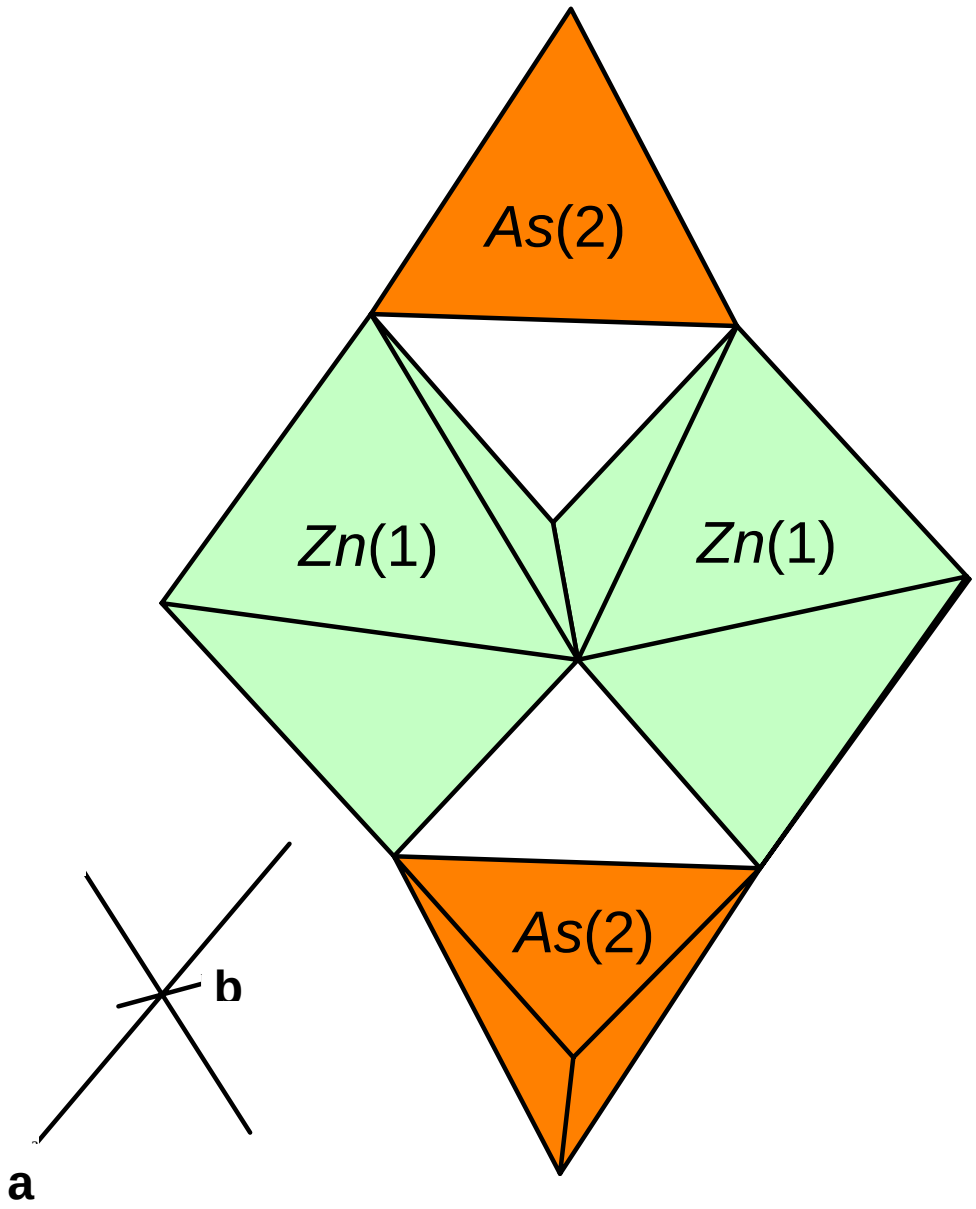

FIGURE 2

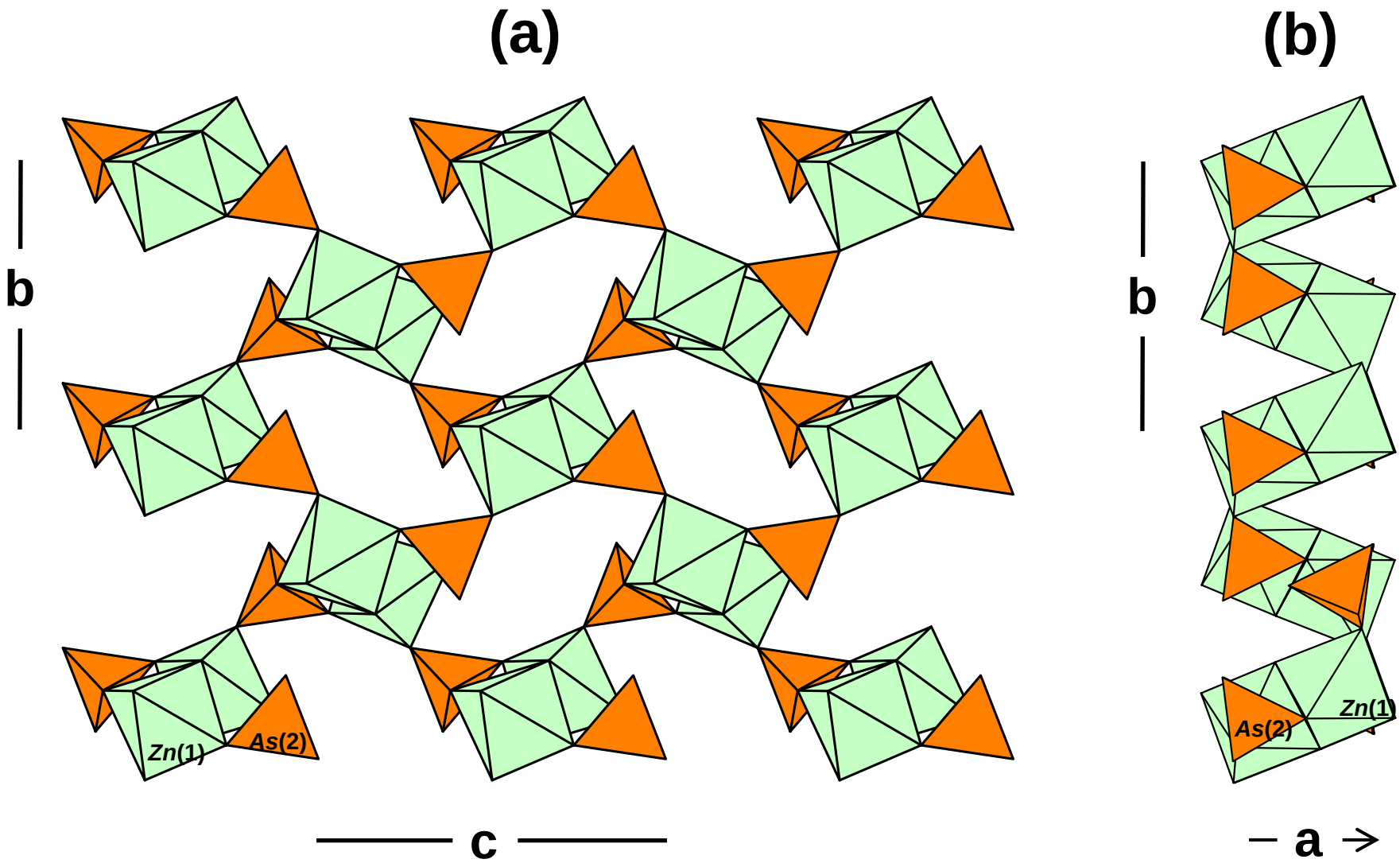

FIGURE 3

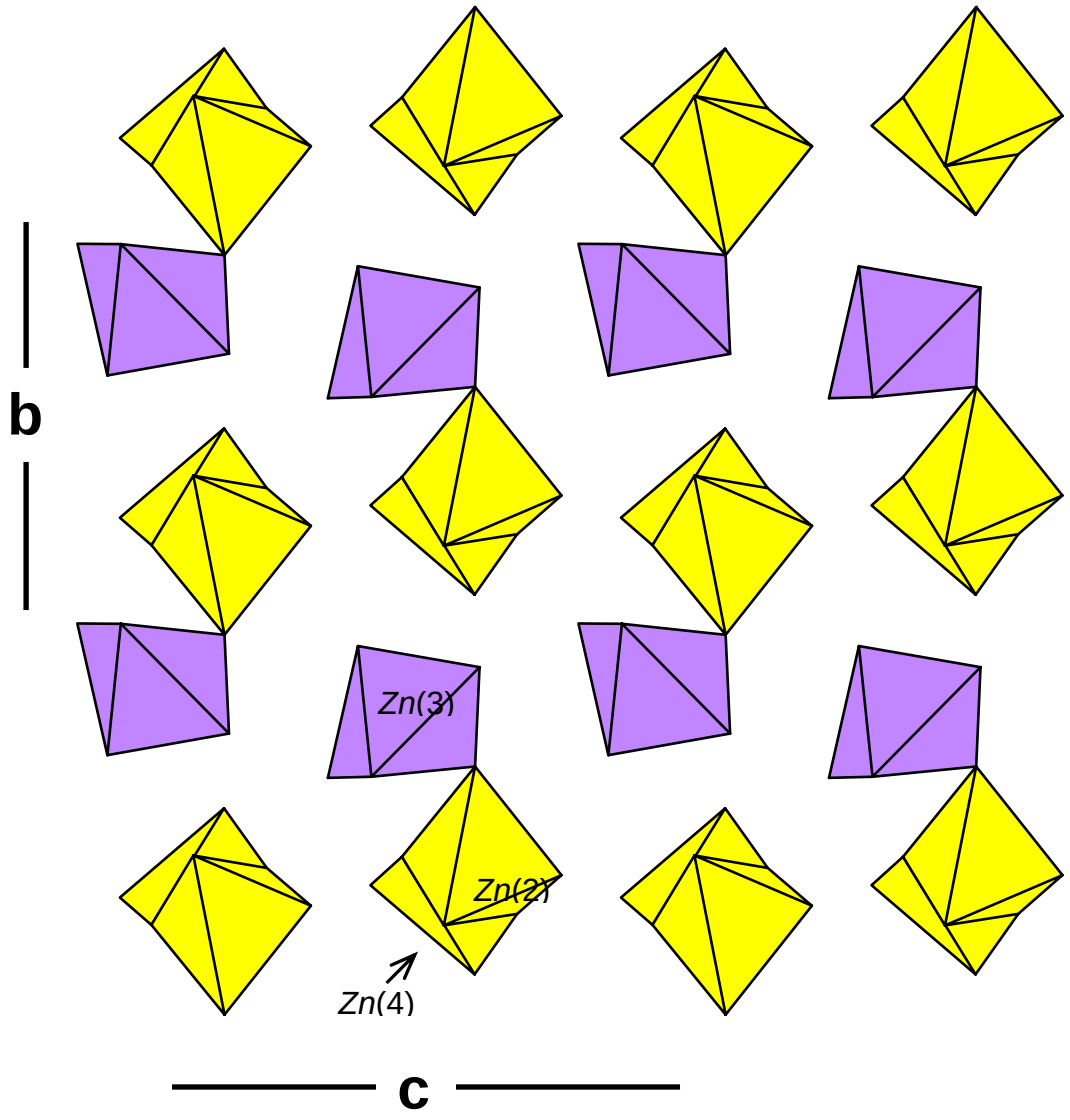

FIGURE 4

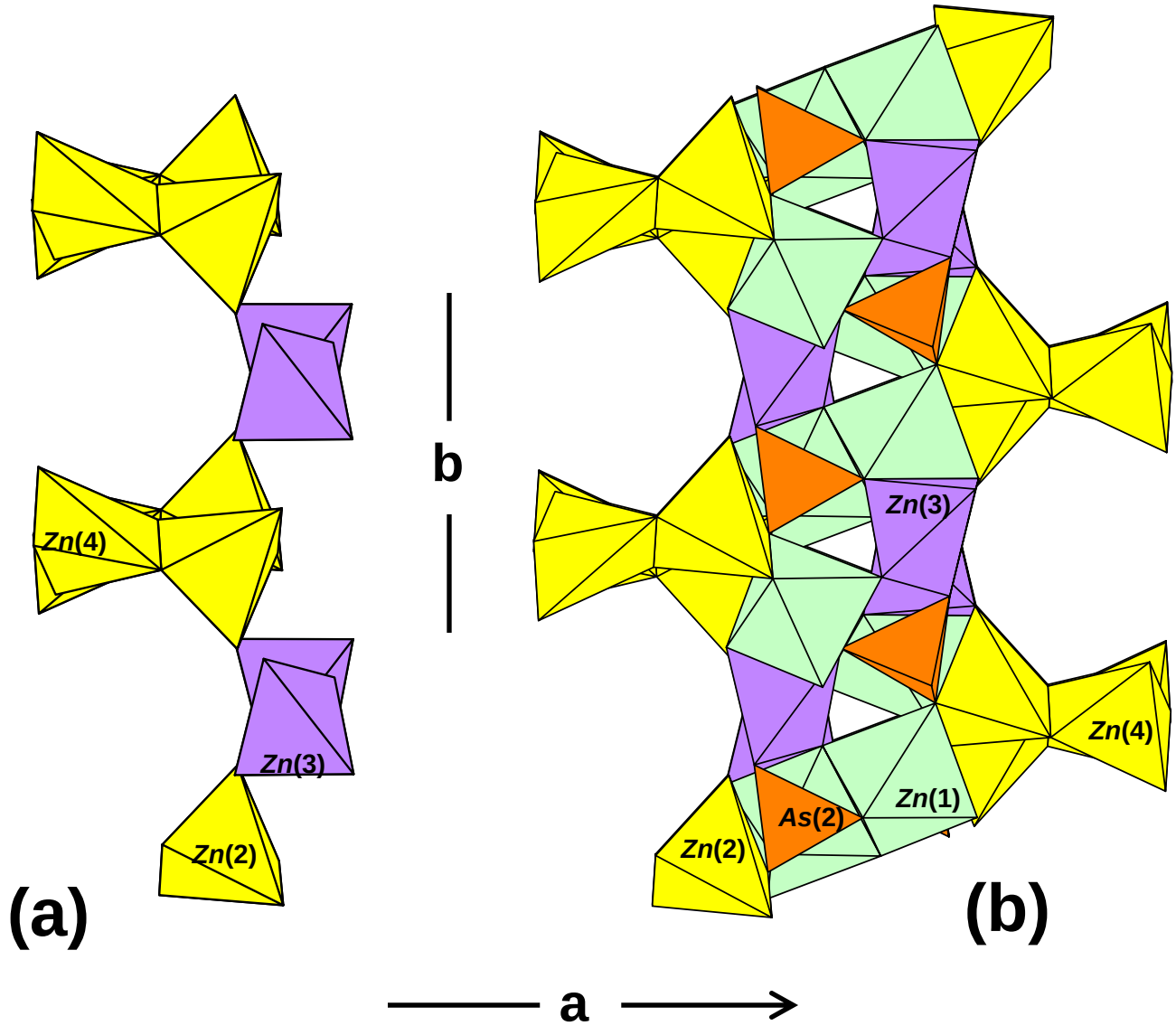

FIGURE 5

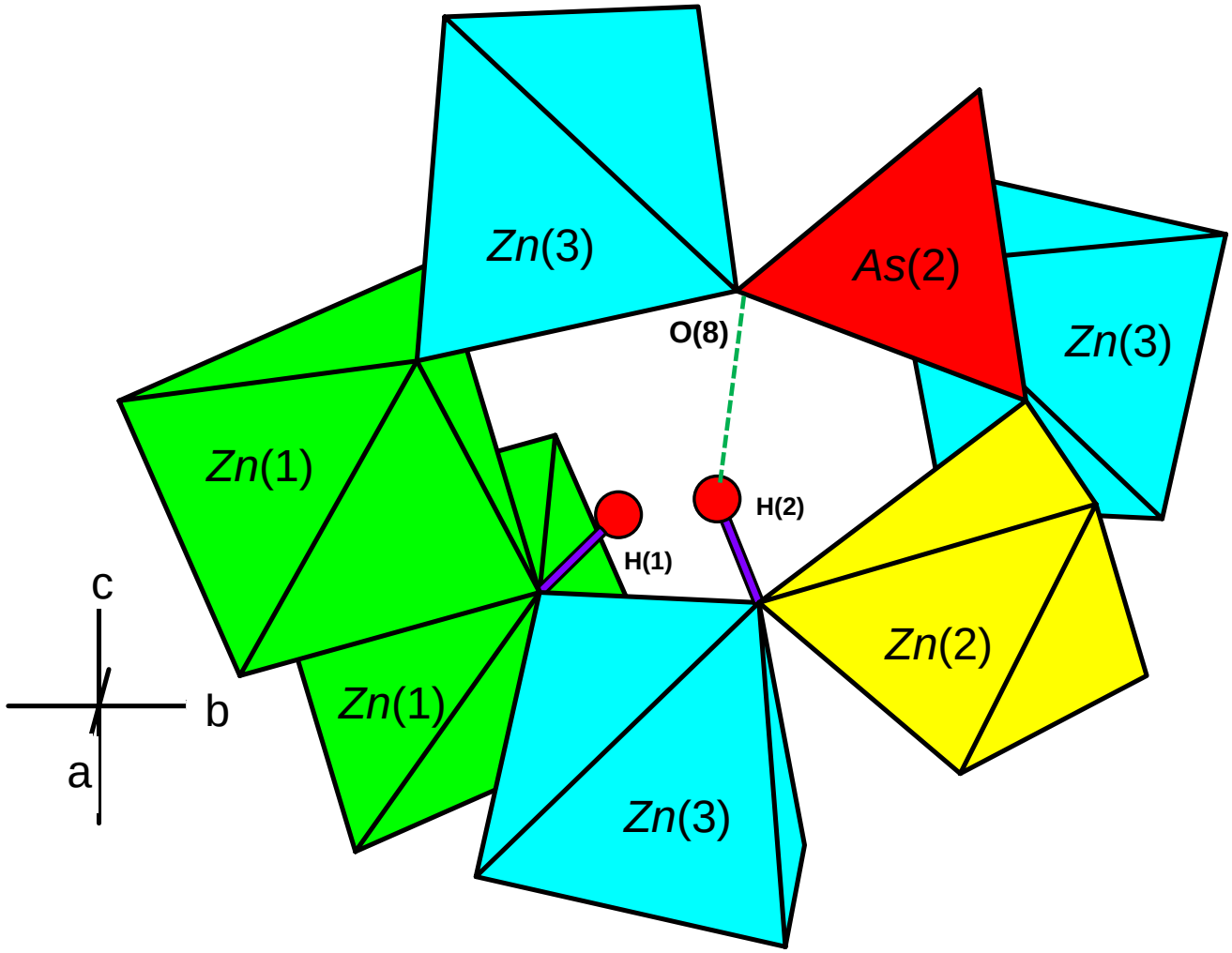

FIGURE 6

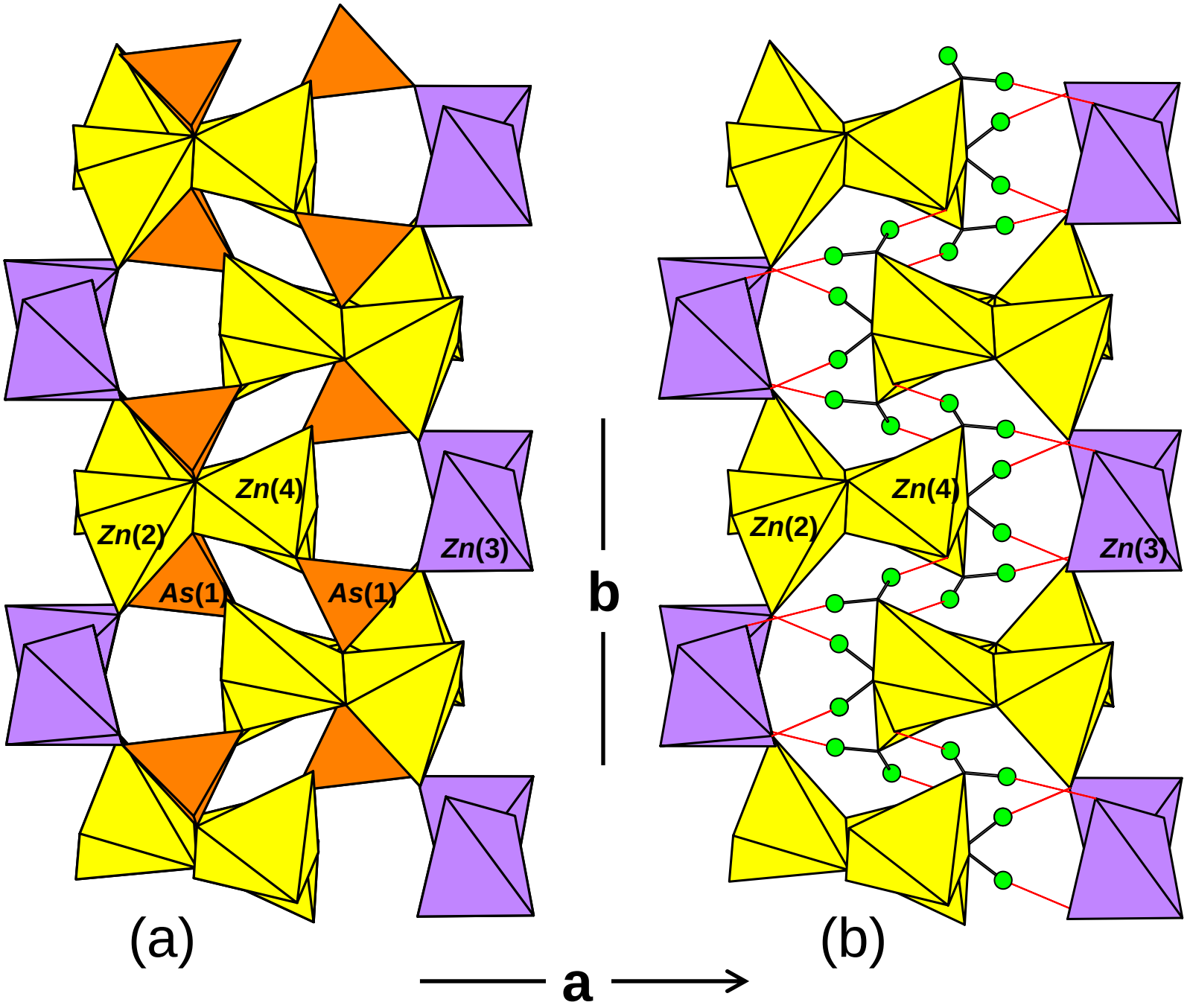

FIGURE 7

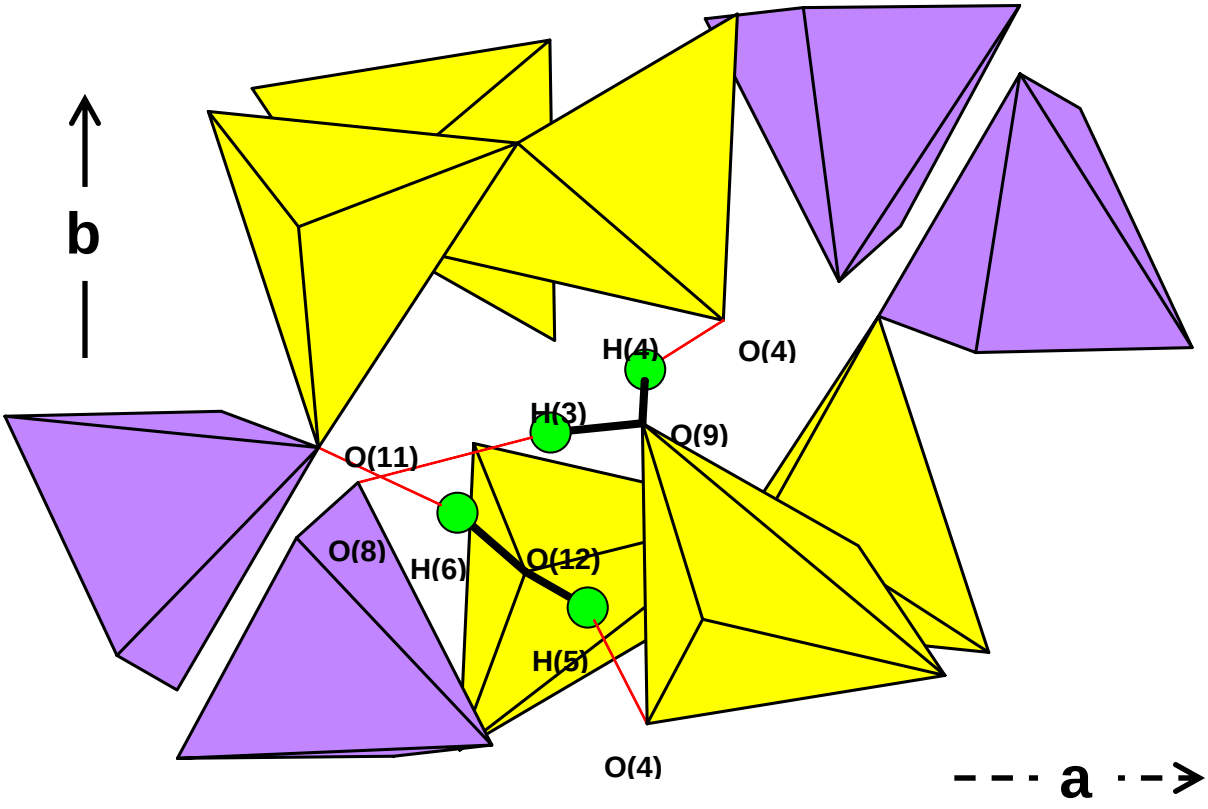

FIGURE 8

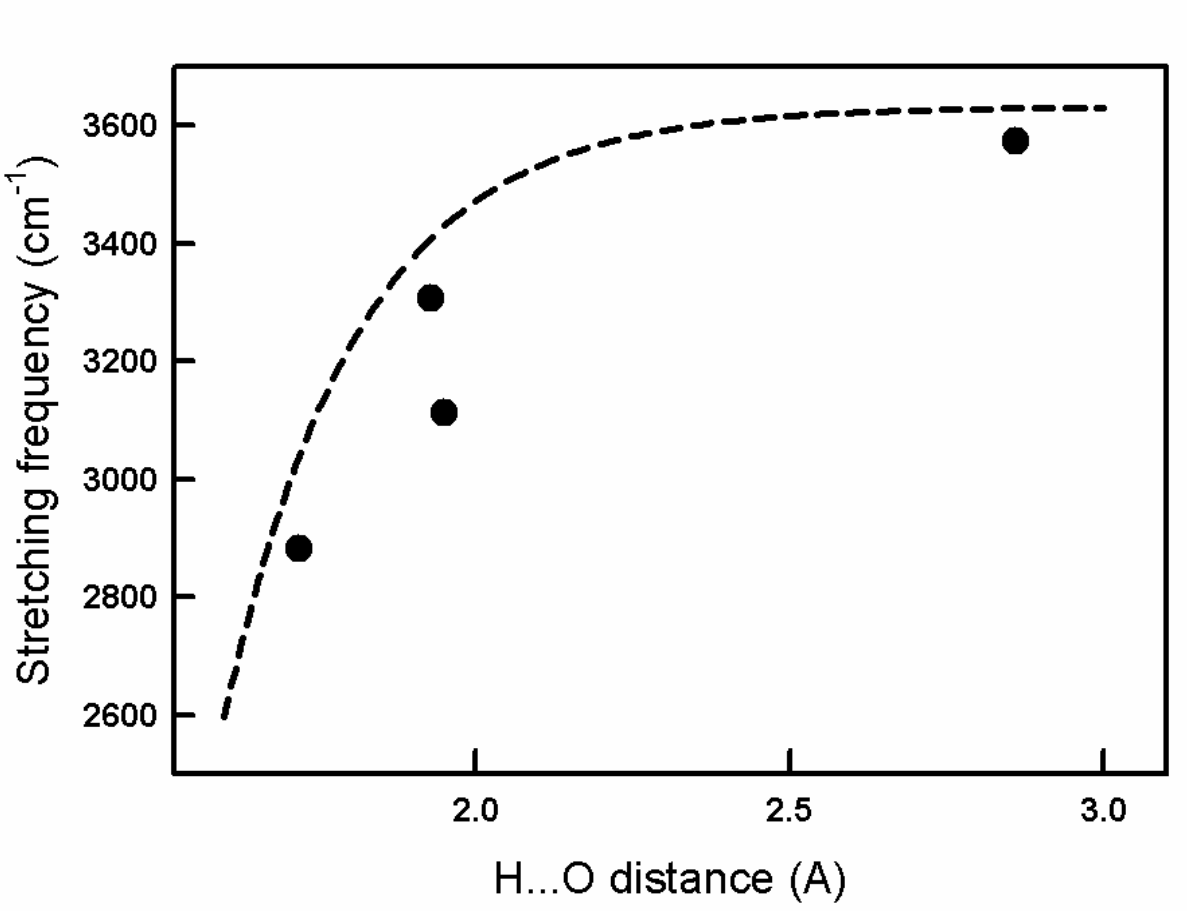
Stretching frequency (cm-1)
3600
3400
3200
3000
2800
2600
2.0
2.5
3.0
H...O distance (A)

FIGURE 9